ISBN: 978-3-95450-261-5 ISSN: 2673-7000 doi: 10.18429/JACoW-NAPAC2025-MOP083

RESONANT CAVITY FOR QUADRUPOLE MOMENT MEASUREMENTS OF HEAVY ION BEAMS*

A. S. Plastun†, S. Cogan, K. Hwang, S. Lidia, T. Maruta, P. N. Ostroumov, S. Zhao, Q. Zhao
Facility for Rare Isotope Beams, Michigan State University, East Lansing, MI, USA

Abstract

Non-invasive and fast beam emittance measurement is highly demanded for accelerated multi-charge-state heavy-ion beams. The driver linac of the Facility for Rare Isotope Beams is the first accelerator capable of accelerating multiple charge states of stripped heavy ion beams and delivering up to 400 kW to the isotope production target. Emittance measurements of, for example, five charge states of uranium beam using conventional wire profile monitors take more than an hour in one location and add up to a few hours throughout the linac. This work presents design studies for a resonant cavity monitor capable of instantaneous measurement of the quadrupole moment of the beam distribution. Coupling with the beam and signal acquisition system, the separation between monopole, dipole, and quadrupole modes of the cavity are discussed.

INTRODUCTION

The driver linac of the Facility for Rare Isotope Beams (FRIB) at Michigan State University is the first accelerator capable of accelerating multiple charge states of stripped heavy-ion beams and delivering up to 400 kW to the isotope production target. Setting up the linac for no-loss acceleration is a challenging problem involving transverse beam matching at several locations in the linac [1,2]. The matching procedure is as follows:

- The beam transverse profiles are measured with a conventional wire scanner for a few different optics settings providing underfocused, focused, and overfocused beam at the wire location, commonly referred to as quadrupole scan.
- Profiles are analyzed to extract the horizontal and vertical rms beam sizes σ_x and σ_y for each measurement.
- Twiss parameters at a given location are found by fitting the beam envelope to the measured data.
- Measurements and fitting are repeated for other charge states of the beam.
- Twiss parameters are loaded to the beam optics code to adjust the magnets' settings for the optimum matching for all charge states of the beam.

Currently, a single wire scan takes about 3 min, which adds up to 25 min for a single-charge-state scan, or 2 h for the five-charge-state uranium beam. Matching in several locations along the linac requires about 4 - 6 h. After implementation of the instant phase setting [3], transverse matching is now one of the most time-consuming procedures in the linac set-up. Since beam species are changed on average every two weeks, expediting the matching procedure is highly demanded at FRIB.

In recent years, we have been working on virtual diagnostics for fast and non-invasive measurements, and reconstruction of Twiss parameters from the beam position monitors' (BPM) data [4, 5]. The reconstruction is based on fitting the beam optics model into the quadrupole terms BPMQ, measured by several BPMs.

$$\mathrm{BPMQ} = G\frac{U_R + U_L - (U_T + U_B)}{U_R + U_L + U_T + U_B} - (x^2 - y^2) \approx \sigma_x^2 - \sigma_y^2, \quad (1)$$

where G is a geometric factor that depends on the BPM geometry, U_T, U_L, U_R and U_B are the induced signal at the top, left, right, and bottom pickups, x and y represent the horizontal and vertical beam centroids. As the primary role of the BPMs is to measure the beam position, the BPMQ is significantly weaker compared to the beam centroid signal. Consequently, small errors, such as calibration inaccuracies, can lead to substantial errors in the measurements. To address these issues, we have developed a machine learning model. Although this model showed a modest improvement over Eq. (1), prediction accuracy cannot exceed the quality of the original data.

The design studies presented in this paper are dedicated to the development of a resonant cavity for the quadrupole term measurements.

RESONANT CAVITY

Resonant beam position monitors are well-known instruments for beam position measurements [6–8]. Several designs have been proposed to measure the second moment of the beam [9]. The principle of resonant monitors is in accumulation of electromagnetic energy that carries the necessary information about the beam distribution by making the cavity resonate at a harmonic of the beam frequency. For example, for the BPMs, the dipole modes of the cavity, and for the second moment monitor, its quadrupole mode is set to resonate with a beam harmonic. The $n\omega_0$ beam current harmonic for Gaussian-shaped bunches of temporal rms length σ and bunch spacing $T = 2\pi/\omega_0$ is presented in Fig. 1 and described as follows [10]:

$$I_n = 2I_0 e^{-(n\omega_0)^2\sigma^2/2}, \quad (2)$$

where I_0 is the average beam current. Shorter bunches have wider spectra, allowing the use of higher harmonics and making the cavities more compact. In this project, we selected the 1288 MHz harmonic ($n = 32$) to be resonant with the quadrupole mode of the rectangular-shaped monitor cavity,

* Work supported by the U.S. Department of Energy, Office of Science, Office of Nuclear Physics under award number DE-SC0025531.
† plastun@frib.msu.edu

ISBN: 978-3-95450-261-5 ISSN: 2673-7000 doi: 10.18429/JACoW-NAPAC2025-MOP083

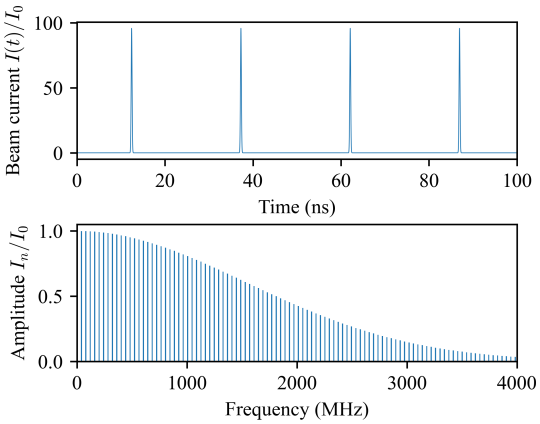

Figure 1: Waveform and spectrum of short Gaussian-shaped bunches. The bunch rate is 40.25 MHz, and the rms bunch length is 52 ps (or 0.75 deg at 40.25 MHz).

as a compromise between the dimensions and the strength of the beam harmonics. Figure 2 shows the patterns of the most important cavity modes and the cavity geometry. The cavity features four quadrupole pins and tapered aperture tubes to enhance the quadrupole mode shunt impedance at the beam velocity $\beta = 0.566$ (200 MeV/u) and fine-tune the modes' frequencies. The main RF parameters of the modes are listed in Table 1. The cavity is equipped with four antenna pickups, which are critically coupled with the quadrupole mode.

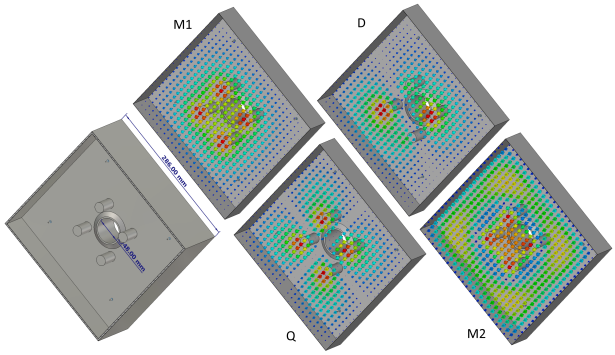

Figure 2: The cavity model (half is shown) and electric field patterns of its modes: (M1) monopole, (D) dipole, (Q) quadrupole, (M2) higher order monopole mode.

Table 1: Modes of the Resonant Cavity Monitor

	M1	D	Q	M2
f_0 (MHz)	623	1025	1288	1620
R/Q (Ω)	116	$4.9e3x^2$	$1.25e7x^4$	1.7
Q_0	19300	19600	17400	21300
Coupl. β	4×0.03	4×0.12	4×0.25	4×1.6

The cavity modes that are parasitic for the quadrupole moment measurement are also known as the *common modes* [6]. There are several ways to suppress the effect of the common modes on the measurements. Frequency discrimination is done by the resonant cavity itself and a narrow-band filter that can be set up in the pickup line.

EQUIVALENT CIRCUIT MODEL

To analyze the response of a cavity mode to a train of beam bunches, we used the equivalent RLC circuit shown in Fig. 3.

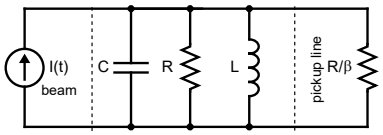

Figure 3: Equivalent circuit diagram for the beam-loaded cavity coupled to a pickup line.

The differential equation describing this circuit is

$$\frac{\dot{I}}{C} = \ddot{V} + \frac{\omega_0 \dot{V}}{Q_L} + \omega_0^2 V, \tag{3}$$

where $\omega_0 = \sqrt{LC}$ is the resonant frequency of the mode, $Q_L = Q_0/(1+\beta) = \omega_0 RC/(1+\beta)$ is the loaded quality factor, β is the coupling factor of the mode and the pickup line. The general solution of Eq. (3) for a single frequency source $I(t) = I_n e^{j\omega t}$ can be written as

$$V(t) = \left[c_1 e^{j\omega_1 t} + c_2 e^{-j\omega_1 t}\right] e^{-t/\tau} + \frac{R I_n e^{j(\omega t+\phi)}}{(1+\beta)\sqrt{1+\gamma^2}}, \tag{4}$$

where c_1 and c_2 are the initial conditions constants, $\omega_1 = \omega_0\sqrt{1-1/(2Q_L)^2}$ and $\tau = 2Q_L/\omega_0$ [11]. The first term represents the signal at the mode's frequency $\omega_1 \approx \omega_0$ decaying with a time constant τ. The second term is a steady-state component oscillating at the frequency of the source, suppressed by the detuning factor $\gamma = Q_L(\omega/\omega_0 - \omega_0/\omega)$, also related to the detuning angle $\phi = -\tan^{-1}\gamma$.

The solution for the resonant harmonic would derive to

$$V(t) = R I_n (1 - e^{-t/\tau}) \cos(\omega_0 t), \tag{5}$$

which is a transient build-up of the field in the cavity. The solution was verified by solving Eq. (3) numerically, assuming a pencil beam at $x = 5$ mm. The FFT-based spectra of the cavity modes shown in Fig. 4 confirm the shock excitation of the common modes at their resonant frequencies and their decay towards the steady state. The signal components of these modes (M1 and M2) at the source frequency remain steady during the simulation time.

MEASUREMENT CIRCUIT

Since the common modes also show up at the quadrupole mode frequency when driven by the beam harmonic, it would be impossible to separate them in the frequency domain. In this case, symmetry-based discrimination is used [6,7]. The signals of each mode are extracted by four antenna pickups, which can be connected via hybrid T's to eliminate the contribution of unwanted modes, as shown in Fig. 5. Another kind of discrimination is done via selective coupling between the modes and the pickup lines. As shown in Table 1, M1 has about 10 times weaker coupling than the Q mode.

ISBN: 978-3-95450-261-5 ISSN: 2673-7000 doi: 10.18429/JACoW-NAPAC2025-MOP083

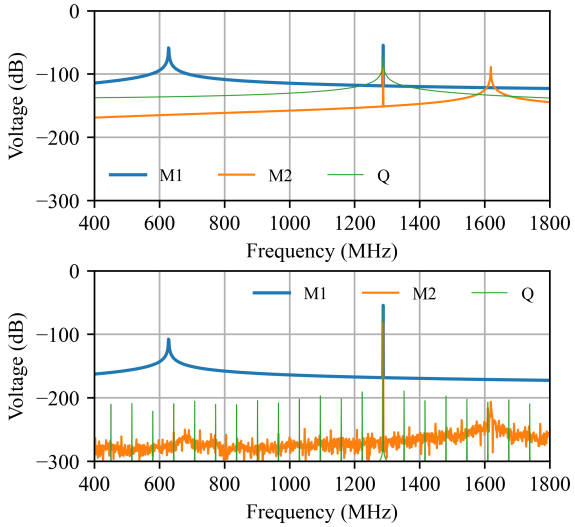

Figure 4: Simulated spectra of the cavity voltage driven by 1288 MHz current harmonic during the first 1000 ns of the transient process (top), and in the steady state (bottom).

The signals induced in the cavity and measured via pickups were simulated with a PIC solver in CST Studio Suite [12], and after combining them in and out of phase, compared to the signals calculated with Eq. (3) numerically. Due to the high computational cost of the PIC simulation, the analysis duration is limited to a few bunches, as can be seen in the waveforms presented in Fig. 6. Thanks to the good agreement between the models, the equivalent circuits can be used to obtain the steady-state solution and estimate the signal strengths. The steady-state waveforms and spectra at a 50 Ω pickup line (before hybrid combiners) obtained numerically from the equivalent circuit model are shown in Fig. 7. The M1 waveform shows the energy exchange between the bunches and the cavity modes. Moreover, the frequency of the M1 signal between the bunches is the resonant frequency of the M1 mode, although it shows up very weak in the spectrum. This is due to the signal phase changes at every bunch arrival, so that over many bunches, this signal component vanishes.

Phase Discrimination

Since the loaded quality factors $Q_L \gg 1$, the detuning angles $\phi \to \pm 90$ deg for the common modes at the quadrupole mode frequency, and $\phi \to 0$ deg for the resonant quadrupole mode. By mixing the 1288 MHz signal from the cavity and a reference 1288 MHz tone (locked in-phase with the beam) in an IQ mixer, one can derive the strength of the quadrupole mode after applying a low-pass filter [7].

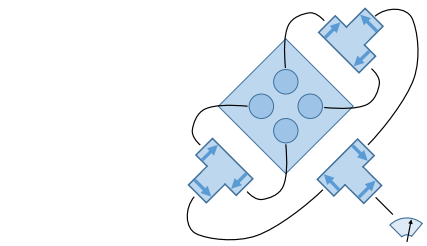

Figure 5: Quadrupole moment measurement circuit via symmetry discrimination using hybrid combiners [9].

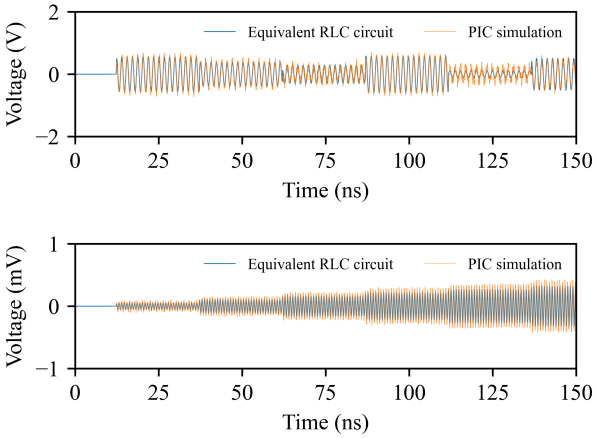

Figure 6: Waveforms of monopole (top) and quadrupole (bottom) modes simulated with PIC solver in CST and calculated numerically for the equivalent circuit.

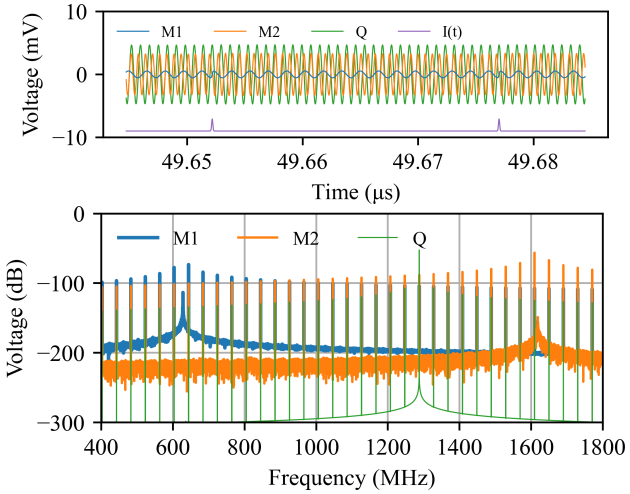

Figure 7: Waveforms and spectra for the steady-state signals in a 50 Ω pickup line calculated numerically for the equivalent circuit.

CONCLUSION

In this paper, we studied several ways to distinguish the quadrupole mode signal from the signals of the common modes obtained from a resonant cavity monitor. These are frequency, symmetry, coupling, and phase discrimination. The study was supported by different types of modeling, including analytical and numerical study of an equivalent circuit model, and an explicit particle-in-cell simulation. The presented models are a great tool for optimizing the cavity geometry and developing the data acquisition and analysis system.

ISBN: 978-3-95450-261-5 ISSN: 2673-7000 doi: 10.18429/JACoW-NAPAC2025-MOP083

REFERENCES

[1] J. Wei *et al.*, "FRIB operations: first three years", in *Proc. 16th International Conference on Heavy Ion Accelerator Technology*, Michigan State University, East Lansing, USA, pp. 1–7, 2025. doi:10.18429/JACoW-HIAT2025-MOX01

[2] T. Maruta *et al.*, "Primary beam development for FRIB experiments", in *Proc. 16th International Conference on Heavy Ion Accelerator Technology*, Michigan State University, East Lansing, USA, pp. 104–109, 2025. doi:10.18429/JACoW-HIAT2025-TUZ02

[3] A. Plastun and P. Ostroumov, "Instant Phase Setting in a Large Superconducting Linac", in *Proc. 5th Int. Particle Accel. Conf. (NAPAC'22)*, Albuquerque, NM, USA, pp. 885–890, 2022. doi:10.18429/JACoW-NAPAC2022-THZD1

[4] K. Hwang *et al.*, "Machine-learning-assisted beam tuning at FRIB", in *Proc. 32nd Linear Accelerator Conference (LINAC2024)*, Chicago, IL, USA, pp. 573–576, 2024. doi:10.18429/JACoW-LINAC2024-THXA004

[5] K. Hwang *et al.*, "Application of ml tools for extraction of bpm-q and transverse beam matching", in *Proc. 16th International Conference on Heavy Ion Accelerator Technology*, Michigan State University, East Lansing, USA, pp. 144–147, 2025. doi:10.18429/JACoW-HIAT2025-TUP11

[6] W. Schnell, "Common-mode rejection in resonant microwave position monitors for linear colliders", CERN, Tech. Rep., 1988. https://cds.cern.ch/record/189450

[7] R. Lorenz, "Cavity beam position monitors", *AIP Conference Proceedings*, vol. 451, no. 1, pp. 53–73, 1998. doi:10.1063/1.57039

[8] D. H. Whittum and Y. Kolomensky, "Analysis of an asymmetric resonant cavity as a beam monitor", *Review of Scientific Instruments*, vol. 70, no. 5, pp. 2300–2313, 1999. doi:10.1063/1.1149756

[9] J. S. Kim, C. D. Nantista, R. H. Miller, and A. W. Weidemann, "Resonant-cavity approach to noninvasive, pulse-to-pulse emittance measurement", *Review of Scientific Instruments*, vol. 76, no. 12, p. 125 109, 2005. doi:10.1063/1.2149191

[10] R. E. Shafer, "Beam position monitoring", *AIP Conference Proceedings*, vol. 212, no. 1, pp. 26–58, 1990. doi:10.1063/1.39710

[11] T. P. Wangler, *RF Linear accelerators*. John Wiley & Sons, 2008.

[12] Dassault Systèmes, *CST Studio Suite*. https://www.3ds.com/products/simulia/cst-studio-suite